The metal–insulator-like and insulator–metal-like behaviors in antimony

2008 J. Phys.: Condens. Matter 20 235232

(http://iopscience.iop.org/0953-8984/20/23/235232)

J. Phys.: Condens. Matter **20** (2008) 235232 (5pp) doi:10.1088/0953-8984/20/23/235232

The metal–insulator-like and insulator–metal-like behaviors in antimony

Z Li, G Li, N L Wang and J L Luo

Beijing National Laboratory for Condensed Matter Physics, Institute of Physics, Chinese Academy of Sciences, Beijing 100080, People's Republic of China

E-mail: jlluo@aphy.iphy.ac.cn

Received 27 February 2008, in final form 14 April 2008
Published 9 May 2008
Online at stacks.iop.org/JPhysCM/20/235232

Abstract

The resistivity and Hall resistivity of semimetallic antimony were measured from 2 to 300 K in magnetic fields up to 14 T. We found that in low field, the resistivity shows metallic behavior. In a modest field, the resistivity decreases to a minimum and then increases with decreasing temperature, showing a metal–insulator-like transition. In high field, the resistivity drops at low temperatures, showing an insulator–metal-like transition. The metal–insulator-like behavior can be explained by the competition of zero field resistivity and magneto-resistance, which is reciprocal to the zero field resistivity. The insulator–metal-like behavior can be explained by the imbalance of two carrier densities which changes the magneto-resistance from being reciprocal to proportional to the zero field resistivity.

(Some figures in this article are in colour only in the electronic version)

1. Introduction

Semimetals, such as bismuth (Bi), antimony (Sb) and graphite, have almost compensated electron and hole densities, which lead to large magneto-resistance(MR) [1]. This large MR has been explained by the two-band model qualitatively for decades [2]. Because semimetals also have low carrier densities, high carrier mobilities and small effective masses, a moderate magnetic field can drive these materials into the quantum regime, where only the lowest Landau level is occupied [3]. So in these materials, it is doubted whether the MR can be explained by conventional two-band theory especially near or in the quantum regime. Recent studies on graphite and Bi reveal some new phenomena which now place the question on the agenda.

Kempa *et al* [4–6] reported a magnetic field-induced metal–insulator (MI)-like behavior in highly oriented pyrolitic graphite (HOPG). The in-plane resistivity changes from a metallic behavior to an insulating-like temperature dependence under a magnetic field above 10 mT. This transition can be scaled with a critical B_c, so there could be an insulating gap opening at the critical field [7, 8]. This change occurs only in the configuration of field perpendicular to the graphite layers [9] and resembles other 2D materials [10–14] which have an MI or insulator-to-superconductor (IS) transition. The two-dimensional limitation has been thought to play an important role. However, graphite single crystals [15] and Bi crystals [16–18] also show similar behavior to HOPG, which excludes dimension effects.

Tokumoto *et al* [19] measured the thermopower of a HOPG and indicates that the material remains metallic when resistivity shows insulating-like temperature dependence, so there is no evidence for the existence of a gap. They found that a simple two-band model can qualitatively describe the MR behavior. Du *et al* [18] also used the conventional multi-band model to fit the longitudinal and transverse resistivity of graphite below 1 T. They derived carrier densities and scattering times, and found a unique inequality of three energy scales in semimetals, $\hbar/\tau \leqslant \hbar\omega_c \leqslant k_B T$, where $\hbar/\tau$ is the width of the energy levels and τ is the electron phonon scattering time, $\hbar\omega_c$ is the cyclotron energy, $k_B T$ is the thermal energy. In a wide interval of temperatures and magnetic fields defined by these energy scales, due to the compensation between electron and hole carriers, the graphite and Bi have the unusual MI-like behavior. Therefore, the MI-like behavior can be interpreted by the conventional theory.

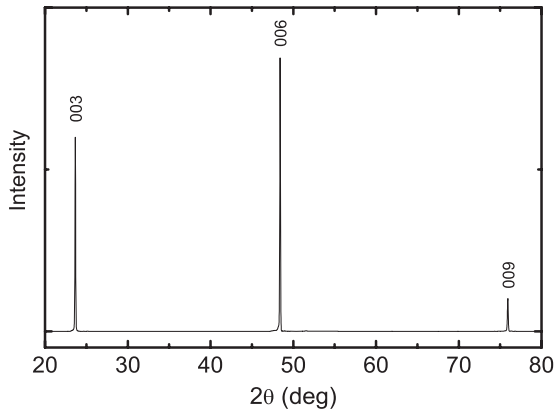

Figure 1. The x-ray diffraction pattern of a single crystal of Sb with surface perpendicular to the *c*-axis.

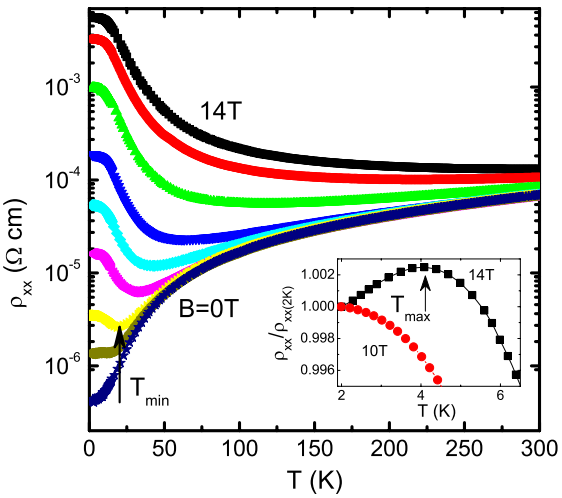

Figure 2. The temperature dependence of in-plane longitudinal resistivity for Sb with the magnetic field along the *c*-axis. From the lowest curve to the highest one, the magnetic fields are 0, 0.1, 0.2, 0.5, 1, 2, 5, 10, and 14 T, respectively. The inset magnifies the low temperature region, and ρ_{xx} is normalized by $\rho_{xx}(2\ \mathrm{K})$. $T_{\min}$ ($T_{\max}$) marks the temperature where ρ_{xx} has a minimum (maximum).

When the magnetic field is increased further, the in-plane resistivity has a maximum with decreasing temperature and then shows metallic behavior which is like a insulator–metal (IM) transition. This behavior is the so-called reentrant metallic behavior [15] which occurs at about 0.2 T for Kish graphite and 4 T for HOPG, and the field at which the reentrant behavior occurs is sample dependent. Bi also shows the reentrant behavior above 0.5 T [17]. Kopelevich *et al* [15, 17] suggested this phenomenon is attributed to field-induced superconductivity which occurs when the system reaches the quantum limit. The quantum Hall effect and Landau-level-quantization-induced superconducting correlation should be considered to account for IM-like behavior. It challenges the conventional two-band theory. However, no clear evidence of superconductivity is observed in these samples under high magnetic fields.

The MI- and IM-like behaviors are novel phenomenon observed in graphite and Bi. It would be interesting to know whether any other semiconductors with similar behaviors exist, and whether these behaviors could be understood within the two-band model. In this paper, we study the resistivity and Hall resistivity of Sb. We have found that Sb, which has a similar crystal and band structure to Bi, also has MI and IM-like behaviors. The carriers densities of Sb are almost T-independent, however the carriers densities of graphite and Bi change obviously with T [20]. So the resistivity of Sb is dominated only by the mobility, which simplifies the discussion. We have found that both MI-and IM-like behaviors can be explained by two-band model.

2. Experimental results and discussion

Crystals with a purity of 99.999% are a commercial product obtained from the 'Beijing General Research Institute for Nonferrous Metals'. Figure 1 shows the x-ray diffraction (XRD) pattern. That only three well indexed sharp peaks can be seen from the XRD pattern indicates that the sample is really a high quality single crystal with lattice parameter $c = 11.27$ Å. The samples for resistivity and Hall resistivity measurements are cleaved from the crystal with surface perpendicular to the *c*-axis. The dimensions of samples are about $2 \times 0.4 \times 0.04$ mm^3. The in-plane resistivity and the Hall resistivity are measured in a Quantum Design physical property measurement system (PPMS) with temperatures down to 2 K and magnetic field up to 14 T. The sample is placed on a rotating sample holder to measure the angular dependence of magneto-resistivity. The Hall voltage was extracted from the antisymmetric parts of the transverse voltages measured under opposite directions, to remove the longitudinal component due to the misalignment of the Hall voltage pads.

Figure 2 shows the temperature dependence of resistivity in the configurations of current $I \perp B$ and $B \parallel c$. In low field, resistivity is metallic and decreases with decreasing temperature T. In a modest field, with decreasing T, the resistivity first decreases and reaches a minimum at $T_{\min}$ and then increases, which is similar to the MI-like behavior observed in graphite and Bi [6, 18]. In a high field, with decreasing T, the resistivity increases and reaches a maximum at $T_{\max}$, and then decreases again (see the inset of figure 2). It is also similar to the IM-like behavior observed in graphene and Bi [17].

The in-plane resistivity versus the angle θ between magnetic field B and current I is shown in figure 3, where B is rotating within the *ab* plane. When $B \parallel I$, i.e. $\theta = 0°$ or 180°, no magneto-resistivity can be discerned. When $B \perp I$, magneto-resistivity reaches a maximum. The curves can be fitted using the formula: $\rho_{xx}(\theta) = \rho_0 + \Delta\rho \sin^2\theta$, where ρ_0 is the zero field resistivity and $\Delta\rho = \rho_{xx}(90°) - \rho_0$. This implies that the magneto-resistivity is dominated by the current I direction, rather than by the crystal axis direction. In the Lorentz-free configuration with $B \parallel I$, there is no Lorentz force on the carriers and there is no magneto-resistance due to orbital effects, which only leaves the spin-related MR which is independent of current direction [17]. However, in this configuration no MR can be discerned. So the MR has

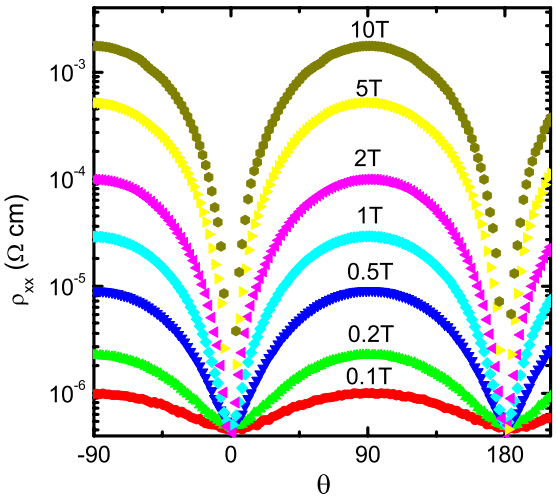

Figure 3. The angular dependence of the resistivity ρ_{xx} at 2 K, with configuration of I in the ab plane and B rotating within the ab plane. θ is the angle between B and I.

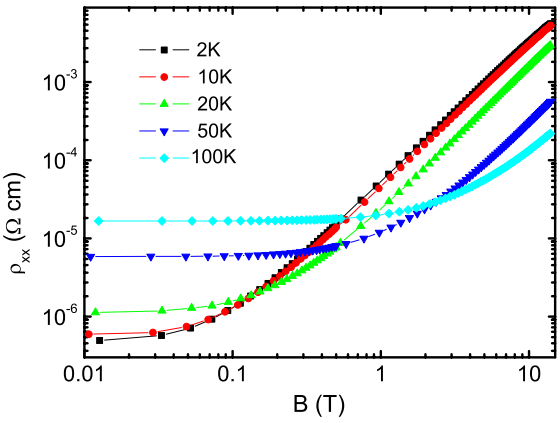

Figure 4. Longitudinal resistivity ρ_{xx} versus applied field B for Sb with the magnetic field along the c-axis.

nothing to do with spin-related effects and is governed by orbital effects.

The temperature dependence MR for a semimetal with two kinds of carriers can be described by the two-band model, where the resistivity can be expressed as [21–23]

$$\rho_{xx} = \frac{\rho_1\rho_2(\rho_1+\rho_2) + (\rho_2/n_1^2 + \rho_1/n_2^2)(B/e)^2}{(\rho_1+\rho_2)^2 + (1/n_1 - 1/n_2)^2(B/e)^2} \quad (1)$$

where $\rho_i = 1/(n_i e\mu_i) = m_i^*/(n_i e^2\tau_i)$ are the resistivity of an electron and hole in zero field, respectively. The parameter μ_i is the mobility, n_i is the carrier density, m_i^* is the effective mass, and τ_i is the relaxation time respectively. The subscript $i = 1, 2$ denotes electron or hole. For Bi and graphite, both the mobilities and carrier densities are temperature dependent. For Sb, the carrier densities are almost temperature independent [20]. Then we can attribute the temperature dependence of resistivity to the temperature dependence of carrier mobility.

For a semimetal, electron and hole densities are almost compensated, so we can assume $n = n_1 = n_2$ to simplify equation (1) into two terms:

$$\rho_{xx} = \frac{\rho_1\rho_2}{(\rho_1+\rho_2)} + \frac{B^2}{n^2e^2(\rho_1+\rho_2)}. \quad (2)$$

The first term is the zero field resistivity $\rho_0 = \rho_1\rho_2/(\rho_1+\rho_2)$, which decreases with decreasing T, (see figure 1). The second term is proportional to B^2, and has an opposite temperature dependence to ρ_0. For a real semimetal, it is proportional to B^p where $1 < p < 2$ [21]. Figure 4 shows the resistivity as a function of field applied along the c-axis. By fitting high field data, we can get $p = 1.8$ for Sb. The resistivity is almost B independent at low field, where the second term is much smaller than ρ_0. With further increase in B, the second term becomes larger than ρ_0, so the resistivity will increase with B. At high temperatures, the resistivity has a large ρ_0, so the high-T curves in figure 4 cross the low-T ones. On the left side of the crossing, the resistivity decreases with decreasing T but on the right side, the resistivity increases with decreasing T. When different temperature curves cross at different field B, there must be a region between two crossings where the resistivity decreases first and then increases with decreasing T, showing MI-like behavior. For example, in figure 4 the 100 and 50 K curves cross at 2 T, then the resistivity at a magnetic field of 1 T is on the left side of the crossing, therefore the resistivity at 1 T decreases from 100 to 50 K. The 50 and 20 K curves cross at 0.5 T, then the resistivity at 1 T is on the right side of the crossing so the resistivity increases from 50 to 20 K. Therefore at 1 T, when temperature decreases from 100 to 20 K, there must be an MI-like behavior, as can be seen in figure 2.

If we assume the electron resistivity is equal to the hole resistivity then $\rho_1 = \rho_2 = 2\rho_0$. Replacing B^2 with $B^{1.8}$ from our experimental result for Sb, equation (2) can have the simple form

$$\rho_{xx} = \rho_0 + \frac{B^{1.8}}{(2ne)^2\rho_0}. \quad (3)$$

The second term of the right side of equation (3) is inversely proportional to its first term ρ_0. So when the resistivity is dominated by the magneto-resistivity, the curve plotted on a logarithmic scale is like a horizontal mirror image of the zero field resistivity ρ_0 (see figure 2 14 T curve and 0 T curve).

In equation (3), we can see ρ_{xx} has a minimum at a temperature $T_{\min}$ where

$$\rho_0(T_{\min}) = B^{0.9}/(2ne). \quad (4)$$

From figure 1, for a given field below 14 T, we have a corresponding $T_{\min}$ at which ρ_{xx} has a minimum value. In figure 5, we plot the $T_{\min}$ as the function of $B^{0.9}/(2ne)$ (closed square), where the carrier density $n = 5.32 \times 10^{25}$ m^{-3} is estimated by Liu *et al* [24]. We also plot zero field resistivity ρ_0 versus the temperature T in the same figure(solid line). It can be seen that all the closed square symbols fall in the T (ρ_0) line. For an example for $B = 0.2$ T, $B^{0.9}/(2ne) = 1.38 \times 10^{-6}$ Ω cm, which is the value of $\rho_0(T)$ at 23 K. This temperature is just where the minimum value of ρ_{xx} at $B = 0.2$ T appears(see figure 1). From the above discussion, the

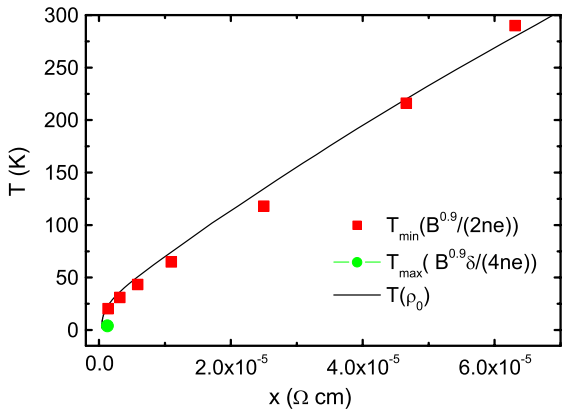

Figure 5. Temperature (T)-reduced magnetic field diagram. $T_{\min}$ and $T_{\max}$ are defined in figure 2. $x = B^{0.9}/(2ne)$) for $T_{\min}(x)$ and $x = B^{0.9}\delta/(ne)$) for $T_{\max}(x)$, where $n = 5.32 \times 10^{25}$ m^{-3} and $\delta = 0.01$. $T(\rho_0)$, which is the inverse function of $\rho_0(T)$, is also plotted for comparison.

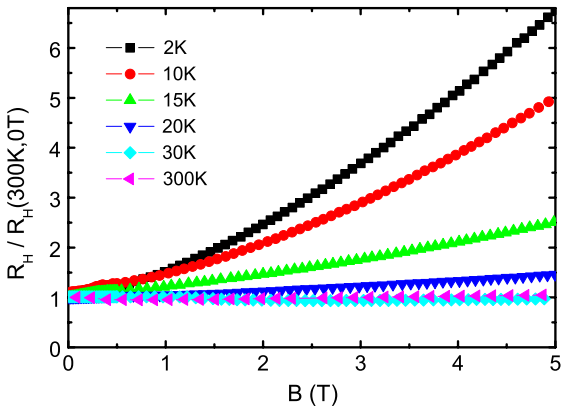

Figure 6. The magnetic field dependence of the Hall coefficient $R_{\rm H}$ which is scaled by the zero field value at 300 K.

two-band model not only can describe the magneto-resistance tendency but also can estimate the temperature at which the MI-like behavior starts to occur.

To explain the IM-like behavior, we need to consider the tiny difference between n_1 and n_2. In the two-band model, the tiny imbalance between the densities of electrons and holes can also change the temperature dependence of resistivity. We can modify equation (1) as

$$\Delta\rho_{xx} = \frac{(\rho_2/n_1 + \rho_1/n_2)^2(B/e)^2}{(\rho_1+\rho_2)^3 + (\rho_1+\rho_2)(1/n_1 - 1/n_2)^2(B/e)^2} \quad (5)$$

where $\Delta\rho_{xx} = \rho_{xx} - \rho_0$. Let us define $\delta = |n_1 - n_2|/n_1$, assume $n = n_1 \approx n_2$, $\rho_1 = \rho_2 = 2\rho_0$, and replace B^2 with $B^{1.8}$ then

$$\frac{1}{\Delta\rho_{xx}} = \frac{4\rho_0 n^2 e^2}{B^{1.8}} + \frac{\delta^2}{4\rho_0}. \quad (6)$$

The competition between the two terms on the right side of equation (6) with increasing field B can explain the IM-like behavior. In low field, the first term is much larger than the second one so $\rho_{xx} \approx \Delta\rho_{xx} \approx B^{1.8}/(4\rho_0 n^2 e^2)$ which is proportional to $1/\rho_0$. When B is large enough, the first term will become smaller than the second term so $\rho_{xx} \approx \Delta\rho_{xx} \approx 4\rho_0/\delta^2$ which is proportional to ρ_0. So $\Delta\rho_{xx}$ must have a maximum with the change of ρ_0. This maximum occurs at $T_{\max}$ where

$$\rho_0 = B^{0.9}\delta/(4ne) \quad (7)$$

Also using $n = 5.32\times10^{25}$ m^{-3} and $\rho_0(2\,{\rm K}) = 4\times10^{-7}\ \Omega$ cm, for $B = 14$ T we can get $|n_1 - n_2|/n = 0.013$. Then if $|n_1 - n_2|/n > 0.013$, $\Delta\rho_{xx}$ has a maximum above 2 K and/or below 14 T. Some experiments and calculations found $n_{\rm e}/n_{\rm p} = 1.01 \sim 1.05$ [24–26], which is sufficient to make $\Delta\rho$ have a maximum below 14 T. However, the difference between the two carrier densities is too small to distinguish precisely due to the experimental error. In addition, Freeman *et al* have suggested that the two carrier densities are equal [27]. The Hall coefficient $R_{\rm H}$ is very sensitive to the carrier imbalance. The two-band model gives [2]

$$R_{\rm H} = -\frac{1}{e}\frac{(\rho_2^2/n_1 - \rho_1^2/n_2) + [(n_1-n_2)/(n_1^2n_2^2)](B/e)^2}{(\rho_1+\rho_2)^2 + [((n_1-n_2)^2/(n_1^2n_2^2](B/e)^2}. \quad (8)$$

If the electron and hole carrier densities are equal, $R_{\rm H}$ should not change with applied field. Figure 6 shows the magnetic field dependence of the Hall coefficient at different temperatures. $R_{\rm H}$ is normalized by its zero field value at 300 K. We can see when temperature is below 20 K, $R_{\rm H}$ deviates from a constant, and the deviation become larger with temperature decreasing. So the difference between electron and hole densities does indeed exist.

For Sb, electron and hole carrier densities are T-independent, so we can assume δ is also T-independent. Therefore, equations (4) and (7) imply that $T_{\min}$ and $T_{\max}$ will have the same B-dependent. In Sb, since $T_{\max}$ happens at very high field, only one $T_{\max}$ data point can be obtained below 14 T in our experiment. This $T_{\max}$ as a function of $B^{0.9}\delta/(ne)$ is plotted in figure 5. Both $T_{\max}$ and $T_{\min}$ can be scaled to the $T(\rho_0)$ curve. In graphite and Bi, although δ changes with temperature, the field dependencies of both $T_{\min}$ and $T_{\max}$ show similar behavior, see figure 3 in [17].

In the above discussion, we only treat the Lorentz effect under magnetic field. Actually, the magnetic field also induces Landau level quantization and make the resistivity show a Shubnikov–de Haas (SdH) oscillation, as seen in figure 7. However, this effect is much smaller than the Lorentz effect, (see figure 4). So the Lorentz effect induced MR is dominant and the SdH oscillation is just a small detail imposed on the MR. Moreover, the existence of the SdH oscillation indicates that Sb is in the metallic state.

The two-band model assumes a spherical Fermi surface which does not agree with the actual material band structure [20, 24, 28]. The effect of carrier interaction, which is important in low carrier density systems and affects the resistivity to some extent [29], is not taken into account either. So the two-band model can explain the trend but fails to fit the resistivity data quantitatively.

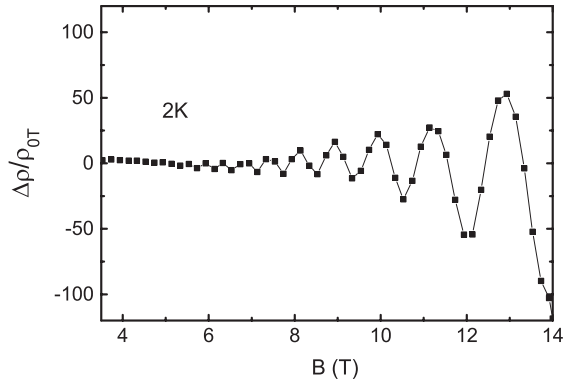

Figure 7. Shubnikov–de Haas oscillations scaled with zero field resistivity versus magnetic field B at 2 K. The background is subtracted after polynomial fitting. The magnetic field B is along the c-axis.

3. Conclusions

In conclusion, the MR of Sb, like that of Bi and graphite, shows both MI-and IM-like behaviors with decreasing temperature. These behaviors can be explained by the classical two-band model. The magnetic field has two effects on resistivity: the MR induced by the Lorentz effect and the SdH oscillation induced by Landau level quantization. In low field or high temperature, these two effects are both smaller than the zero field resistivity, so the resistivity is dominated by the zero field resistivity and shows metallic behavior. In modest field and temperature, the resistivity is dominated by the Lorentz effect, the MR is larger than the zero field resistivity, so the resistivity shows an insulator-like behavior. In high field and low temperature, although the SdH oscillation appears, the Lorentz effect is much larger than the Landau level effect, so the resistivity is still dominated by the Lorentz effect. However, the carrier imbalance becomes dominant in the two-band model equation and changes the resistivity from an insulator-like behavior to a metallic behavior.

Acknowledgments

The authors would like to acknowledge the helpful discussions with Professor T Xiang. This work is supported by the National Science Foundation of China, the Knowledge Innovation Project of Chinese Academy of Sciences, and 973 project under grant No. 2006CB921300.

References

[1] Lovett D R 1977 *Semimetals and Narrow-Bandgap Semiconductors* vol 107 ed H J Goldsmith and D W G Ballentyne (London: Pion) p 170
[2] Ziman J M 1960 *Electrons and Phonons: The Theory of Transport Phenomena in Solids* ed N F Mott, E C Bullard and D H Wilkinson (Oxford University Press) p 490
[3] Williamson S J, Foner S and Dresselhaus M S 1965 *Phys. Rev.* **140** A1429
[4] Kopelevich Y, Lemanov V V, Moehlecke S and Torres J H S 1999 *Phys. Status Solidi* **41** 2135
[5] Kempa H, Kopelevich Y, Mrowka F, Torres J H S, Hohne R and Esquinazi P 2000 *Solid State Commun.* **115** 539
[6] Kempa H, Esquinazi P and Kopelevich Y 2002 *Phys. Rev.* B **65** 241101(R)
[7] Khveshchenko D V 2001 *Phys. Rev. Lett.* **87** 206401
[8] Khveshchenko D V 2001 *Phys. Rev. Lett.* **87** 246802
[9] Kempa H, Semmelhack H C, Esquinazi P and Kopelevich Y 2003 *Solid State Commun.* **125** 1
[10] Liu Y, McGreer K A, Nease B, Haviland D B, Martinez G, Halley J W and Goldman A M 1991 *Phys. Rev. Lett.* **67** 2068
[11] Wang T, Clark K P, Spencer G F, Mack A M and Kirk W P 1994 *Phys. Rev. Lett.* **72** 709
[12] Yazdani A and Kapitulnik A 1995 *Phys. Rev. Lett.* **74** 3037
[13] Shahar D, Tsui D C, Shayegan M, Bhatt R N and Cunningham J E 1995 *Phys. Rev. Lett.* **74** 4511
[14] Kravchenko S V, Simonian D, Sarachik M P, Mason W and Furneaux J E 1996 *Phys. Rev. Lett.* **77** 4938
[15] Kopelevich Y, Torres J H S, da Silva R R, Mrowka F, Kempa H and Esquinazi P 2003 *Phys. Rev. Lett.* **90** 156402
[16] Yang F Y, Liu K, Hong K, Reich D H, Searson P C and Chien C L 1999 *Science* **248** 1335
[17] Kopelevich Y, Pantoja J C M, da Silva R R and Moehlecke S 2006 *Phys. Rev.* B **73** 165128
[18] Du X, Tsai S.-W, Maslov D L and Hebard A F 2005 *Phys. Rev. Lett.* **94** 166601
[19] Tokumoto T, Jobiliong E, Choi E S, Oshima Y and Brooks J S 2004 *Solid State Commun.* **129** 599
[20] Issi J P 1979 *Aust. J. Phys.* **32** 585
[21] Wilson A H 1954 *The Theory of Metals* (Cambridge: Cambridge University Press)
[22] Ziman J M 1964 *Principles of the Theory of Solids* (Cambridge: Cambridge University Press)
[23] Callway J 1991 *Quantum Theory of the Solid State* 2nd edn (New York: Academic)
[24] Liu Y and Allen R E 1995 *Phys. Rev.* B **52** 1566
[25] Windmiller L R 1966 *Phys. Rev.* **149** 472
[26] Ketterson J and Eckstein Y 1963 *Phys. Rev.* **132** 1885
[27] Freeman S J and Juretschke H J 1961 *Phys. Rev.* **124** 1379
[28] Sugawara K, Sato T, Souma S, Takahashi T and Suematsu H 2006 *Phys. Rev.* B **73** 045124
[29] Kukkonen C A and Maldague P F 1979 *Phys. Rev.* B **19** 2394